PHYSICAL REVIEW A 78, 061604(R) (2008)

# Coherent energy manipulation in single-neutron interferometry

S. Sponar,[1] J. Klepp,[1,2] R. Loidl,[1] S. Filipp,[1] G. Badurek,[1] Y. Hasegawa,[1,3] and H. Rauch[1]
[1]*Atominstitut der Österreichischen Universitäten, 1020 Vienna, Austria*
[2]*Institut Laue-Langevin, Boîte Postale 156, F-38042 Grenoble Cedex 9, France*
[3]*PRESTO, Japan Science and Technology Agency (JST), Kawaguchi, Saitama, Japan*
(Received 5 December 2007; published 15 December 2008)

We have observed the stationary interference oscillations of a triple-entangled neutron state in an interferometric experiment. Time-dependent interaction with two radio-frequency fields enables coherent manipulation of an energy degree of freedom in a single neutron. The system is characterized by a multiply entangled state governed by a Jaynes-Cummings Hamiltonian. The experimental results confirm coherence of the manipulation as well as the validity of the description.

DOI: 10.1103/PhysRevA.78.061604 PACS number(s): 03.75.Dg, 03.65.Ud, 07.60.Ly, 42.50.Dv

Since the pioneering work of Einstein, Podolsky, and Rosen [1] numerous experiments have exploited the concept of nonlocality, which tests local hidden-variable theories (LHVTs). The LHVTs are a subset of a larger class of hidden-variable theories, namely, the noncontextual hidden-variable theories (NCHVTs). Noncontextuality implies that the value of a measurement is independent of the experimental context, i.e., of previous or simultaneous measurements [2,3]. Noncontextuality is a more stringent demand than locality because it requires mutual independence of the results for commuting observables even if there is no spacelike separation [4].

In the case of neutron experiments, entanglement is not achieved between particles, but between different degrees of freedom. Since the observables in different Hilbert spaces commute with each other, the single-neutron system is suitable for studying NCHVTs. Single-particle entanglement, between the spinor and the spatial part of the neutron wave function [5], as well as full tomographic state analyses [6], have already been accomplished. In addition, the contextual nature of quantum theory [7] has been demonstrated using neutron interferometry [8]. Aiming at the preparation of a single-particle multiply entangled state, implementation of another degree of freedom to be entangled with the neutron's spin and path degrees of freedom was a challenge.

The neutron's energy seems to be an almost ideal candidate for this third degree of freedom, due to its experimental accessibility within a magnetic resonance field [9]. For this purpose the time evolution of the system is described by a photon-neutron state vector, which is an eigenvector of the corresponding modified Jaynes-Cummings (JC) Hamiltonian [10,11]. The JC Hamiltonian can be adopted for a system consisting of a neutron coupled to a quantized radio-frequency (rf) field [12].

This Rapid Communication reports on observation of stationary interference patterns, confirming coherent energy manipulation of the neutron wave function. This technique provides realization of triple entanglement between the neutron's path, spin, and energy degrees of freedom.

Since two rf fields, operating at frequencies $\omega$ and $\omega/2$, are involved in the actual experiment, the modified corresponding JC Hamiltonian is denoted as

$$\mathcal{H}_{\mathrm{JC}} = -\frac{\hbar^2}{2m}\nabla^2 - \mu B_0(\mathbf{r})\sigma_z + \hbar\left(\omega a_\omega^\dagger a_\omega + \frac{\omega}{2}a_{\omega/2}^\dagger a_{\omega/2}\right) + \mu\left(\frac{B_1^{(\omega)}(\mathbf{r})}{\sqrt{N_\omega}}(a_\omega^\dagger\tilde{\sigma} + \mathrm{H.c.}) + \frac{B_1^{(\omega/2)}(\mathbf{r})}{\sqrt{N_{\omega/2}}}(a_{\omega/2}^\dagger\tilde{\sigma} + \mathrm{H.c.})\right) \tag{1}$$

with $\tilde{\sigma}=\frac{1}{2}(\sigma_x+i\sigma_y)$. The first term accounts for the kinetic energy of the neutron. The second term leads to the usual Zeeman splitting of $2|\mu|B_0$. The third term adds the photon energy of the oscillating fields of frequencies $\omega$ and $\omega/2$, by use of the creation and annihilation operators $a^\dagger$ and $a$. Finally, the last term represents the coupling between photons and the neutron, where $N_{\omega_j}=\langle a_{\omega_j}^\dagger a_{\omega_j}\rangle$ represents the mean number of photons with frequencies $\omega_j$ in the rf field. Note that the first two and the last terms concern the spatial $|\psi(\mathbf{r})\rangle$ and the (time-dependent) energy $|E(t)\rangle$ subspaces of neutrons, respectively [13].

The state vectors of the oscillating fields are represented by coherent states $|\alpha\rangle$, which are eigenstates of $a^\dagger$ and $a$. The eigenvalues of coherent states are complex numbers, so one can write $a|\alpha\rangle=\alpha|\alpha\rangle=|\alpha|e^{i\phi}|\alpha\rangle$ with $|\alpha|=\sqrt{N}$. Using Eq. (1) one can define a total state vector including not only the neutron system $|\Psi_{\mathrm{N}}\rangle$, but also the two quantized oscillating magnetic fields: $|\Psi_{\mathrm{i}}\rangle=|\alpha_\omega\rangle\otimes|\alpha_{\omega/2}\rangle\otimes|\Psi_{\mathrm{N}}\rangle$. In a perfect Si-crystal neutron interferometer the wave function behind the first plate, acting as a beam splitter, is a linear superposition of the sub-beams belonging to the right ($|\mathrm{I}\rangle$) and the left ($|\mathrm{II}\rangle$) paths, which are laterally separated by several centimeters. The sub-beams are superposed at the third crystal plate and the wave function in the forward direction then reads $|\Psi_{\mathrm{N}}\rangle\propto|\Psi_{\mathrm{N}}^{(\mathrm{I})}\rangle+|\Psi_{\mathrm{N}}^{(\mathrm{II})}\rangle$, where $|\Psi_{\mathrm{N}}^{(\mathrm{I})}\rangle$ and $|\Psi_{\mathrm{N}}^{(\mathrm{II})}\rangle$ differ only by an adjustable phase factor $e^{i\chi}$ ($\chi=N_{\mathrm{ps}}b_c\lambda D$, with the thickness of the phase shifter plate $D$, the neutron wavelength $\lambda$, the coherent scattering length $b_c$, and the particle density $N_{\mathrm{ps}}$ in the phase shifter plate). By rotating the plate, $\chi$ can be varied systematically. This yields the well-known intensity oscillations of the two beams emerging behind the interferometer, usually denoted as O and H beams [8]. A sketch of the setup, split up into regions numbered from 1 on the left to 6 on the right side, is depicted in Fig. 1.

In our experiment, only the beam in path II is exposed to

 

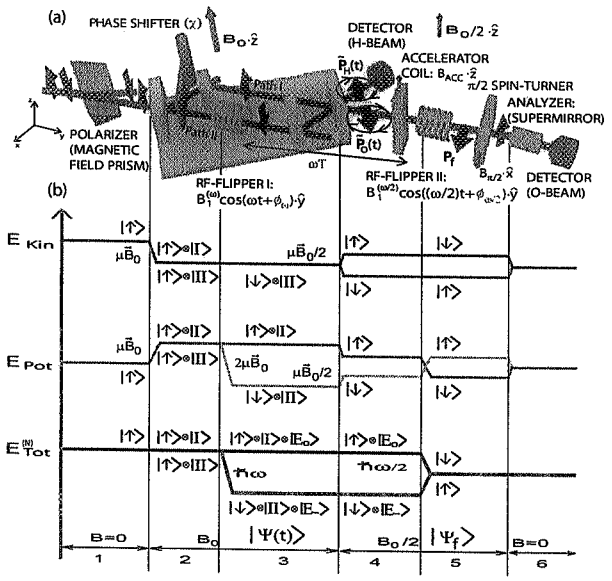


FIG. 1. (Color online) (a) Schematic view of the experimental setup for stationary observation of interference between two rf fields, showing the arrangement of two radio-frequency flip coils (the first within one path of the skew-symmetric Mach-Zehnder-type neutron interferometer and the other driven by the half frequency behind the interferometer), accelerator coil, and $\pi/2$ spin turner. Appropriate spin analysis of the neutron beam allows measurement of relative phase shifts. (b) Energy level diagram of the two interfering sub-beams $|\mathrm{I}\rangle$, $|\mathrm{II}\rangle$ during their passage through the different static field regions ($B_0$, $B_0/2$, and $B=0$), including corresponding spin states $|\uparrow\rangle$, $|\downarrow\rangle$ and taking into account the spin flips at rf frequencies $\omega$ and $\omega/2$.

the rf field of frequency $\omega$, resulting in a spin-flip process in region 3. The spin-flip configuration of the first rf field ensures an entanglement of the spin and spatial degrees of freedom of the neutron state [5]. Interacting with a time-dependent magnetic field, the total energy of the neutron is no longer conserved after the spin flip [14–18]. Photons of energy $\hbar\omega$ are exchanged with the rf field. This particular behavior of the neutron is described by the dressed-particle formalism [12,19]. Consequently, the two sub-beams $|\mathrm{I}\rangle$ and $|\mathrm{II}\rangle$ now differ in total energy [see Fig. 1(b)]. Therefore the neutron state can be considered to consist of the three subsystems, namely, the total energy, path, and spin degrees of freedom. In principle, a spin-independent energy manipulation of neutrons is also possible: for instance, the up- and the down-spin wave packets, separated by the so-called longitudinal Stern-Gerlach effect [20,21], undergo successive fast-activated dc-rf and rf-dc flippers, respectively, resulting in a positive energy shift.

A coherent superposition of $|\mathrm{I}\rangle$ and $|\mathrm{II}\rangle$ results in the multiply entangled dressed state vector, expressed as

$$|\Psi(t)\rangle \propto |\alpha_\omega\rangle \otimes |\alpha_{\omega/2}\rangle \otimes \frac{1}{\sqrt{2}}(|\mathrm{I}\rangle \otimes |E_0\rangle \otimes |\uparrow\rangle + e^{i\chi}|\mathrm{II}\rangle \otimes e^{i\omega t}|E_0 - \hbar\omega\rangle \otimes e^{i\phi_\omega}|\downarrow\rangle), \quad (2)$$

where $|\uparrow\rangle$, $|\downarrow\rangle$ denote the neutron's up and down spin states

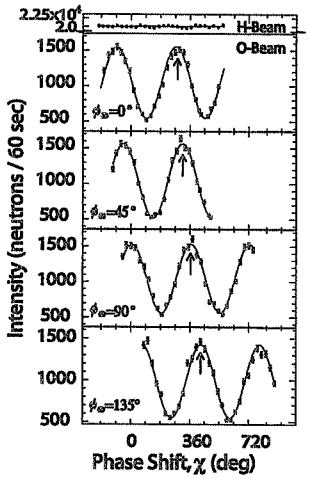


FIG. 2. Typical interference patterns of the H and the O beam. In the H beam no interference fringes are observed due to orthogonal spin states in the interfering sub-beams, whereas the O beam exhibits time-independent sinusoidal intensity oscillations, when the phase shifter plate ($\chi$) is rotated. A phase shift occurs on varying $\phi_\omega$.

referred to the chosen quantization axis. The state vector of the neutron acquires a phase $\pm\phi_\omega$ during the interaction with the oscillating field, given by $B(t)=B_1\cos(\omega t+\phi_\omega)$, induced by the action of the operators $a_\omega$ and $a_\omega^\dagger$ in the last term of Eq. (1). The neutron part of the total state vector is represented by a path-energy-spin entanglement within a single neutron system. At the last plate of the interferometer (region 4) the two sub-beams are recombined, which is described by the projection operator $\hat{O}^{(\mathrm{P})}=\frac{1}{2}(|\mathrm{I}\rangle+|\mathrm{II}\rangle)(\langle\mathrm{I}|+\langle\mathrm{II}|)$. Due to the orthogonality of the energy and spin eigenstates, the polarization is zero and no intensity modulations are observed in the H beam, which is plotted in Fig. 2. A time-resolved measurement (see [9]) can reveal the dynamic behavior of the polarization, expressed as

$$\tilde{\mathbb{P}}_{\mathrm{O}}(t) = [\cos(\chi - \omega t - \phi_\omega), \sin(\chi - \omega t - \phi_\omega), 0]. \quad (3)$$

This phenomenon has been measured separately [9], and is related to the spinor precession known from zero-field spin-echo experiments [15,16].

The beam recombination is followed by an interaction with the second rf field, with half frequency $\omega/2$, in region 5. Mathematically the energy transfer is represented by the operator $\hat{O}^{(\mathrm{E})}=(1/\sqrt{2})|E_0-\hbar\omega/2\rangle(\langle E_0|+\langle E_0-\hbar\omega|)$, respectively. The total state vector is given by

$$|\Psi_{\mathrm{f}}\rangle \propto |\alpha_\omega\rangle \otimes |\alpha_{\omega/2}\rangle \otimes (|\mathrm{I}\rangle + |\mathrm{II}\rangle) \otimes |E_0 - \hbar\omega/2\rangle \otimes \frac{1}{\sqrt{2}}(e^{i\phi_{\omega/2}}|\downarrow\rangle + e^{i\omega T}e^{i\chi}e^{i(\phi_\omega-\phi_{\omega/2})}|\uparrow\rangle), \quad (4)$$

where $\phi_\omega$ and $\phi_{\omega/2}$ are the phases induced by the two rf fields and $\omega T$ is the zero-field phase, with $T$ being the neutron s propagation time between the two rf flippers [22]. The energy difference between the orthogonal spin states is compensated by choosing a frequency of $\omega/2$ for the second rf

flipper, resulting in a stationary state vector. Hence the time dependence of the polarization vector is eliminated:

$$\mathbb{P}_f = (\cos \Delta_{tot}, \sin \Delta_{tot}, 0), \quad (5)$$

where $\Delta_{tot}=(\chi-2\phi_{\omega/2}+\phi_\omega+\omega T)$ consists of the phases induced by the path (phase shifter $\chi$), spin (phases of the two rf fields $\phi_\omega$, $\phi_{\omega/2}$), and energy manipulation (zero-field phase $\omega T$). The principle of energy compensation is visualized in Fig. 1(b). As seen from $\Delta_{tot}$ in Eq. (5), each of the three degrees of freedom can be manipulated independently and the associated observables are separately measurable.

The arrangement of two rf flippers of frequencies $\omega$ and $\omega/2$ can be interpreted as an interferometer scheme for the neutron's total energy. Due to energy splitting, the first rf flipper generates a superposition of two coherent energy states, similar to the action of the first beam splitter of a Mach-Zehnder interferometer, where a single beam is split spatially into two coherent sub-beams. The second flipper compensates the energy difference and therefore acts as a beam analyzer equivalent to the last beam splitter of the interferometer.

After applying a projection operator $\hat{P}^{(S)}=|\uparrow\rangle\langle\uparrow|$ to the spin (region 6), the stationary interference oscillations are given by $I_0 \propto 1+\nu\cos(\chi+\Phi+\omega T)$, introducing the fringe visibility $\nu$ and the relative phase $\Phi$. The relative phase can be calculated as $\Phi=\phi_\omega-2\phi_{\omega/2}$. In the following experiment we demonstrate the coherence property of the modified JC manipulation defined in Eq. (1) as well as the phase dependence expressed above.

The experiment was carried out at the neutron interferometer instrument S18 at the high-flux reactor of the Institute Laue-Langevin in Grenoble, France. A monochromatic beam, with mean wavelength $\lambda_0=1.91$ Å ($\Delta\lambda/\lambda_0\sim0.02$) and $5\times5$ mm$^2$ beam cross section, is polarized by a birefringent magnetic field prism in the $\hat{z}$ direction [23] [see Fig. 1(a), region 1]. In a nondispersive arrangement of the monochromator and the interferometer crystal angular separation can be used such that only the spin-up (or spin-down) component satisfies the Bragg condition at the first interferometer plate (beam splitter) in region 2. Behind the beam splitter the neutron s wave function is found in a coherent superposition of $|\Psi_N^{(I)}\rangle$ and $|\Psi_N^{(II)}\rangle$, and only $|\Psi_N^{(II)}\rangle$ passes the first rf flipper mounted in one path of the interferometer. Acting like a typical NMR arrangement, rf flippers require two magnetic fields: A static field $\mathbb{B}_0\cdot\hat{z}$ with $B_0=\hbar\omega_{rf}/(2|\mu|)$ and a perpendicular oscillating field $\mathbb{B}_1^{(\omega)}\cos(\omega t+\phi_\omega)\cdot\hat{y}$ with amplitude $B_1^{(\omega)}=\pi\hbar/(2\tau|\mu|)$, where $\mu$ is the magnetic moment of the neutron and $\tau$ is the time the neutron requires to traverse the rf field region. The oscillating field is produced by a water-cooled rf coil with a length of 2 cm, operating at a frequency of $\omega/2\pi=58$ kHz. The static field is provided by the uniform magnetic guide field $B_0\sim2$ mT, which is produced by a pair of water-cooled Helmholtz coils. However, outside the rf coil the Larmor precession around the static magnetic guide field induces an additional phase.

The two sub-beams are recombined at the third plate (region 4) resulting in a time-dependent state vector due to the different energies of the two partial wave functions. Since the two superposed spin states are orthogonal, no intensity modulation is observed, as seen at the H detector. In contrast, the O beam (forward direction) passes the second rf flipper, operating at half the frequency of the first rf flipper. The oscillating field is denoted as $\mathbb{B}_1^{(\omega/2)}\cos[(\omega/2)t+\phi_{\omega/2}]\cdot\hat{y}$, and the strength of the guide field was tuned to about 1 mT in order to satisfy the frequency resonance condition.

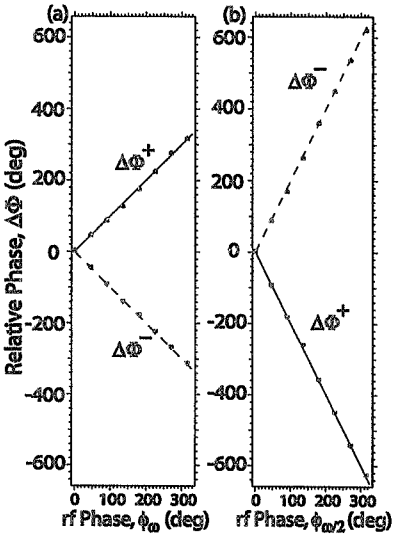


FIG. 3. Relative phase $\Delta\Phi^\pm$ vs (a) $\phi_\omega$ and (b) $\phi_{\omega/2}$. The sign of the phase depends on the chosen initial polarization.

This flipper compensates the energy difference between the two spin components, by absorbtion and emission of photons of energy $E=\hbar\omega/2$. The phases of the two guide fields and the zero-field phase $\omega T$ were compensated by an additional Larmor precession within a tunable accelerator coil with a static field, pointing in the $\hat{z}$ direction. Finally, the spin is rotated back to the $\hat{z}$ direction by use of a $\pi/2$ static field spin turner, and analyzed along the $\hat{z}$ direction due to spin-dependent reflection within a Co-Ti multilayer supermirror. Typical interference patterns are depicted in Fig. 2. In the O beam a fringe contrast of 52.4(2)% was achieved, whereas no oscillation was observed in the H detector, where no further manipulations were applied.

It is possible to invert the initial polarization simply by rotating the interferometer by a few seconds of arc, thereby selecting the spin-down component to enter the interferometer, which is expected to lead to an inversion of the relative phase. In order to observe a relative phase shift, in practice it is necessary to perform a reference measurement. This is achieved by turning off the rf flipper inside the interferometer, thus yielding the relative phase difference $\Delta\Phi^\pm = \pm\phi_\omega \mp 2\phi_{\omega/2}$, where $\pm$ denotes the respective initial spin orientation. Figure 3(a) shows a plot of the relative phase $\Delta\Phi^\pm$ versus $\phi_\omega$, with $\phi_{\omega/2}=0$, and a phase shift $\Delta\Phi^\pm$ caused by a variation of $\phi_\omega$. As expected, the slope is positive for initial spin up orientation [1.007(8)], and negative for the spin-down case [−0.997(5)]. In Fig. 3(b) $\phi_{\omega/2}$ is varied, while $\phi_\omega$ is kept constant, yielding slopes of −1.995(8) and 1.985(7), depending again on the initial beam polarization.

At this point the geometric nature of $\Delta\Phi^\pm$ should be emphasized. Within the rf flipper that is placed inside the inter-

ferometer, the neutron spin traces a semi-great-circle from $|\uparrow\rangle$ to $|\downarrow\rangle$ on the Bloch sphere and returns to its initial state $|\uparrow\rangle$ when passing the second rf flipper. This procedure is repeated along different semi-great-circles when varying $\phi_\omega$ or $\phi_{\omega/2}$, respectively. The two semi-great-circles enclose an angle $\phi_\omega - \phi_{\omega/2}$ and hence a solid angle $\Omega = 2(\phi_\omega - \phi_{\omega/2})$. The solid angle $\Omega$ yields a pure geometric phase $\Phi_G^{\pm} = \Omega/2$, as in [24,25].

Our work can be seen within a framework related to tripartite entanglement. There are two nonequivalent classes of tripartite entanglement represented by the Greenberger-Horne-Zeilinger (GHZ) state [26,27] and the $W$ state [28] when the three quantum subsystems have nonlocal correlations. Classification of a GHZ-like state in a single-neutron system will be the subject of forthcoming work. In addition, we claim that preparation of other types of triple entanglement can be realized using neutron interferometry and spin precession. For instance, creation of a $W$ state can be achieved with rf flippers within a double-loop interferometer. It is worth noting that the operation of the rf flipper within the interferometer could be interpreted as a "controlled-NOT-NOT gate," with path as the control qubit and energy and spin as target qubits.

In summary, we have established a technique of coherent energy manipulation, by utilizing the neutron interferometer in combination with two rf fields to observe time-independent interference patterns. Energy splitting provides an additional degree of freedom, available for multiple entanglement of path, spin, and energy of the neutron. Our data verify theoretical predictions and illustrate the significance of single-particle entanglement.

This work has been partly supported by the Austrian Science Foundation, FWF (Grants No. P17803-N02 and No. F1513). Y.H. would like to thank the Japan Science and Technology Agency (JST) for financial support.

[1] A. Einstein, B. Podolsky, and N. Rosen, Phys. Rev. **47**, 777 (1935).
[2] J. S. Bell, Rev. Mod. Phys. **38**, 447 (1966).
[3] N. D. Mermin, Rev. Mod. Phys. **65**, 803 (1993).
[4] C. Simon, M. Zukowski, H. Weinfurter, and A. Zeilinger, Phys. Rev. Lett. **85**, 1783 (2000).
[5] Y. Hasegawa, R. Loidl, G. Badurek, M. Baron, and H. Rauch, Nature (London) **425**, 45 (2003).
[6] Y. Hasegawa, R. Loidl, G. Badurek, S. Filipp, J. Klepp, and H. Rauch, Phys. Rev. A **76**, 052108 (2007).
[7] Y. Hasegawa, R. Loidl, G. Badurek, M. Baron, and H. Rauch, Phys. Rev. Lett. **97**, 230401 (2006).
[8] H. Rauch and S. A. Werner, *Neutron Interferometry* (Clarendon, Oxford, 2000).
[9] G. Badurek, H. Rauch, and J. Summhammer, Phys. Rev. Lett. **51**, 1015 (1983).
[10] E. T. Jaynes and F. W. Cummings, Proc. IEEE **51**, 89 (1963).
[11] B. W. Shore and P. L. Knight, J. Mod. Opt. **40**, 1195 (1993).
[12] E. Muskat, D. Dubbers, and O. Schärpf, Phys. Rev. Lett. **58**, 2047 (1987).
[13] Factorization of wave functions is a common technique, e.g., to solve time-independent Schrödinger equations.
[14] R. Golub, R. Gähler, and T. Keller, Am. J. Phys. **62**, 779 (1994).
[15] R. Gähler and R. Golub, Phys. Lett. A **123**, 43 (1987).
[16] S. V. Grigoriev, W. H. Kraan, and M. T. Rekveldt, Phys. Rev. A **69**, 043615 (2004).
[17] B. Alefeld, G. Badurek, and H. Rauch, Z. Phys. B: Condens. Matter **41**, 231 (1981).
[18] J. Summhammer, K. A. Hamacher, H. Kaiser, H. Weinfurter, D. L. Jacobson, and S. A. Werner, Phys. Rev. Lett. **75**, 3206 (1995).
[19] J. Summhammer, Phys. Rev. A **47**, 556 (1993).
[20] N. Arend, R. Gähler, T. Keller, G. Georgii, T. Hills, and P. Böni, Phys. Lett. A **327**, 21 (2004).
[21] B. Alefeld, G. Badurek, and H. Rauch, Phys. Lett. **83A**, 32 (1981).
[22] S. Sponar, J. Klepp, G. Badurek, and Y. Hasegawa, Phys. Lett. A **372**, 3153 (2008).
[23] G. Badurek, R. J. Buchelt, G. Kroupa, M. Baron, and M. Villa, Physica B **283**, 389 (2000).
[24] A. G. Wagh, G. Badurek, V. C. Rakhecha, R. J. Buchelt, and A. Schricker, Phys. Lett. A **268**, 209 (2000).
[25] A. Shapere and F. Wilcek, *Geometric Phases in Physics*, Advanced Series in Mathematical Physics Vol. 5 (World Scientific, Singapore, 1989).
[26] D. M. Greenberger, M. A. Horne, and A. Zeilinger, in *Bell's Theorem, Quantum Theory, and Concepts of the Universe*, edited by M. Kafatos (Kluwer Academic, Dordrecht, The Netherlands, 1989).
[27] D. M. Greenberger, A. Shimony, M. A. Horne, and A. Zeilinger, Am. J. Phys. **58**, 1131 (1990).
[28] W. Dür, G. Vidal, and J. I. Cirac, Phys. Rev. A **62**, 062314 (2000).